



# Determination of empirical parameters for root water uptake models

Marcos Alex dos Santos<sup>1</sup>, Quirijn de Jong van Lier<sup>2</sup>, Jos C. van Dam<sup>3</sup>, and Andre Herman Freire Bezerra<sup>1</sup>

<sup>1</sup>"Luiz de Queiroz" College of Agriculture, University of São Paulo, Piracicaba (SP), Brazil

<sup>2</sup>Center for Nuclear Energy in Agriculture, University of São Paulo, Piracicaba (SP), Brazil

<sup>3</sup>Department of Environmental Sciences, Wageningen University, The Netherlands

*Correspondence to:* Marcos Alex dos Santos (marcosalex.ma@gmail.com)

**Abstract.** Detailed physical models describing root water uptake (RWU) are an important tool for the prediction of RWU and crop transpiration, but involved hydraulic parameters are hardly-ever available, making them less attractive for many studies. Empirical models are more readily used because of their simplicity and lower data requirements. The purpose of this study is to evaluate the capability of some empirical models to mimic the RWU distribution under varying environmental conditions predicted from numerical simulations with a detailed physical model. A review of some empirical models used as sub-models in ecohydrological models is presented, and alternative empirical RWU models are proposed. The parameters of the empirical models are determined by inverse modelling of simulated depth-dependent RWU. The simulated scenarios give more insight into the behaviour of the physical model, especially under wet soil conditions and high potential transpiration rate. The performance of the empirical models and their optimized empirical parameters depend on the scenario. The largely used empirical RWU model by Feddes only performs well in scenarios with low root length density  $R$ , i.e. for the scenarios of low RWU “compensation”. For medium and high  $R$ , the Feddes RWU model cannot mimic properly the root uptake dynamics as predicted by the physical model. The RWU model by Jarvis provides good predictions only for low and medium  $R$  scenarios. For high  $R$ , the Jarvis model cannot mimic the uptake patterns predicted by the physical model. Incorporating a newly proposed reduction in the Jarvis model improved RWU predictions. The proposed models are more capable of predicting similar RWU patterns by the physical model. The statistical indices point them as the best alternatives to mimic RWU predictions by the physical model.

## 1 Introduction

The rate at which a crop transpires depends on atmospheric conditions, the shape and properties of the boundary between crop and atmosphere, the root system geometry, and crop and soil hydraulic properties. The study and modelling of the involved interactions is motivated by the importance of transpiration for global climate and crop growth (Chahine, 1992) as well as by the role root water uptake (RWU) plays in soil water distribution (Yu et al., 2007). The common modelling approach introduced by Gardner (1960), referred to as microscopic or mesoscopic (Raats, 2007), is not readily applicable to practical problems due to the difficulty in describing the complex geometrical and operational function of root system and its complex interactions



with soil (Passioura, 1988). However, it gives insight into the process and allows developing upscaled- physical macroscopic models (De Willigen and van Noordwijk, 1987; Heinen, 2001; Raats, 2007; De Jong van Lier et al., 2008, 2013).

In many one- and two-dimensional problems, macroscopic RWU is modelled as a sink term in the Richards equation, whose dependency on water content or pressure head is usually represented by simple empirical functions (ex. Feddes et al. (1976, 5 1978); Lai and Katul (2000); Li et al. (2001); Vrugt et al. (2001); Li et al. (2006)). Most of these models are derived from the Feddes et al. (1978) model, which consists of partitioning potential transpiration over depth according to root length density and applying a stress reduction function of piecewise linear shape — defined by five threshold empirical parameters — to account for local uptake reduction. Results of experimental studies (Arya et al., 1975b; Green and Clothier, 1995, 1999; Vandoorne et al., 2012) and the development of physically based-models (De Jong van Lier et al., 2008; Javaux et al., 2008) have helped 10 in understanding the mechanism of RWU as a non-local process affected by non-uniform soil water distribution (Javaux et al., 2013). Accordingly, a plant can increase water uptake in wetter soil layers in order to compensate for uptake reductions in dryer layers to keep transpiration rate at potential rate or mitigate transpiration reduction. Several empirical approaches have been developed over the years to account for this so-called compensation mechanism (Jarvis, 1989; Li et al., 2002, 2006; Lai and Katul, 2000). These models have been incorporated into larger hydrological models and tested at site-specific environments, 15 showing improved predictions for, e.g., soil water content and crop transpiration (ex. Braud et al. (2005); Yadav et al. (2009); Dong et al. (2010)). Comparisons with physically-based models (Jarvis, 2011; de Willigen et al., 2012) implicitly accounting for compensation showed that models that do not account for compensation, like Feddes et al. (1978), are less accurate with respect to crop transpiration and soil water content predictions.

Recently, De Jong van Lier et al. (2013) developed a mechanistic model for predicting water potentials along the soil-root- 20 leaf pathway, allowing the prediction of RWU and crop transpiration. This model was incorporated in the eco-hydrological model SWAP (Van Dam et al., 2008) by employing a piece-wise function between leaf pressure head and relative transpiration, reducing the number of empirical parameters compared to other relations (ex. Fisher et al. (1981)). Besides parameters describing soil hydraulic properties and root geometry, this new model requires information about root radial hydraulic conductivity, xylem axial conductance and a limiting leaf water potential. Although conceptually interesting, the difficulty to obtain the 25 required input parameters makes the model less attractive for routine applications.

Empirical RWU models are more readily used because of their relative simplicity and lower data requirements. On the other hand, their empirical parameters do not have a clear physical meaning and cannot be independently measured. Their limitations under varying environmental conditions are quite incomprehensible and not well established. For the case of the Feddes et al. (1978) transpiration reduction function, indeed, threshold values are available in literature (Taylor and Ashcroft, 30 1972; Doorenbos and Kassam, 1986) for some crops and some levels of transpiration demand. Nevertheless, experimental (Denmead and Shaw, 1962; Zur et al., 1982) and theoretical (Gardner, 1960; De Jong Van Lier et al., 2006) studies indicate that these parameters do not depend only on crop type and atmospheric demand, but are also determined by root system parameters and soil hydraulic properties. Furthermore, there are only very few analyses of the validity of these values, and they cannot be used for other models (ex. the Jarvis (1989) model) due to differences in model concepts. Therefore, more 35 accurate values for crops accounting for more environmental factors are necessary in order to apply these models in wider



scenarios. Due to the great number of models developed over the years, it is paramount to investigate some of these models before attempting to determine their parameters.

The general purpose of this study is to evaluate the capability of some empirical models to mimic the dynamics of RWU distribution under varying environmental conditions performed in numerical experiments with a detailed physical model (De Jong van Lier et al., 2013). The detailed physical model accounts for resistances from the soil to the leaf. We first review some empirical RWU models that have been employed in ecohydrological models and suggest some alternatives. By determining the parameters of the empirical models by inverse modelling of simulated depth-dependent RWU, it becomes clear to which extent the empirical models can mimic the dynamic patterns of RWU.

## 2 Theory

RWU and crop transpiration are linked through the continuity principle for water flow in the soil-plant-atmosphere pathway:

$$T_a = \int_{z_m} S(z) dz \quad (1)$$

where  $T_a$  (L) is the crop transpiration and  $S$  ( $L^3 L^{-3} T^{-1}$ ) is the root water uptake, dependent on crop properties and soil hydraulic conditions, a function of soil depth  $z$  (L), and  $z_m$  (L) the maximum rooting depth. Eq. 1 neglects the change of water storage in the plant, which is justified for daily scale predictions, assuming that plants rehydrate to the same early morning water potentials on successive days (Taylor and Klepper, 1978).

In a macroscopic modelling approach, RWU is calculated as a sink term  $S$  in the Richards equation, which for the vertical coordinate is given by:

$$\frac{\partial \theta}{\partial t} = \frac{\partial}{\partial z} \left[ K(\theta) \left( \frac{\partial h}{\partial z} + 1 \right) \right] - S \quad (2)$$

where  $\theta$  ( $L^3 L^{-3}$ ) is the soil water content,  $h$  (L) the soil water pressure head,  $K$  ( $L T^{-1}$ ) the soil hydraulic conductivity,  $t$  (T) the time and  $z$  (L) the vertical coordinate (positive upward). To apply eq. 2, an expression for  $S$  is needed. Physical equations in analogy to Ohm's law have been suggested (see the review of Molz (1981) for examples) as well as expressions derived by upscaling microscopic models (De Willigen and van Noordwijk, 1987; Feddes and Raats, 2004; De Jong van Lier et al., 2008, 2013). Alternatively, simple empirical models requiring less information about plant and soil hydraulic properties have also been proposed and are more commonly used. Most of these models use the Feddes approach (Feddes et al., 1976, 1978), formulated as:

$$S(z) = S_p(z) \alpha(h[z]) \quad (3)$$

where  $\alpha(h)$  is the RWU reduction function, defined by Feddes et al. (1978) as a piece-wise linear function of  $h$  (Fig. 1). According to this approach, a reduction in  $S$  due to  $\alpha(h[z]) < 1$  directly implies a transpiration reduction, making  $\alpha(h)$  to be called as transpiration reduction function.  $S_p$  is the potential RWU, which is determined by partitioning potential transpiration



$T_p$  over depth. Several ways to estimate  $S_p$  have been proposed (Prasad, 1988; Li et al., 2001; Raats, 1974; Li et al., 2006), but it is most common to distribute  $T_p$  according to the fraction of root length density  $R$  ( $L^3L^{-3}$ ):

$$S_p(z) = \frac{R(z)}{\int_{z_m} R(z) dz} T_p = \beta(z) T_p \quad (4)$$

where  $\beta$  ( $L^{-1}$ ) is the normalized root length density.

- 5 Different functions to calculate  $\alpha$  have been suggested, normally considering  $\alpha$  a function of  $\theta$  (ex. Lai and Katul (2000); Jarvis (1989)), of  $h$  (ex. Feddes et al. (1978)) or of a combination of both (Li et al., 2006). Using  $h$  seems to be more feasible because of its relation to soil water energy and the fact that obtained parameters of such a function would be more likely applicable to different soils. Some reduction functions, generally associated to reservoir models for soil water balance, correlates RWU to the effective saturation. Regarding the shape of the reduction curve, they can be smooth non-linear functions
- 10 constrained between wilting point and saturation or piece-wise linear functions, but they all have more than one empirical parameter. The parameters of the smooth non-linear functions allow easy curve fitting, whereas in the piece-wise functions they stand for the threshold at which RWU (or crop transpiration) is reduced due to drought stress, which has been an important parameter in crop water management.

Metselaar and De Jong van Lier (2007) showed that for a vertically homogeneous root system the shape of  $\alpha$  is linearly

15 related nor to soil water content neither to pressure head. A linear relation to the matric flux potential, a composite soil hydraulic function defined in eq. 5, is physically more plausible and was experimentally shown by Casaroli et al. (2010). Matric flux potential is defined as

$$M = \int_{h_w}^h K(h) dh \quad (5)$$

where  $h_w$  is the soil pressure head at wilting point. Accordingly, a more suitable expression for  $\alpha$  would be a piece-wise linear

20 function of  $M$  (Fig. 1). RWU can then be calculated by the Feddes model (eq. 3) by replacing its reduction function for water deficit by the alternative illustrated in Fig. 1.

## 2.1 Physically based root water uptake model

By upscaling earlier findings (De Jong Van Lier et al., 2006; Metselaar and De Jong van Lier, 2007) of water flow towards a single root in the microscopic scale disregarding plant resistance to water flow, De Jong van Lier et al. (2008) derived the

25 following expression for  $S$ :

$$S(z) = \rho(z)(M_s(z) - M_0) \quad (6)$$

where  $M_s$  is the bulk soil matric flux potential,  $M_0$  the value of  $M$  at root surface and  $\rho(z)$  ( $L^{-2}$ ) a composite parameter, depending on  $R$  and root radius  $r_0$ :

$$\rho(z) = \frac{4}{r_0^2 - a^2 r_m^2(z) + 2[r_m^2(z) + r_0^2] \ln[ar_m(z)/r_0]} \quad (7)$$



where  $r_m (= \sqrt{1/\pi R})$  (L) is the rhizosphere radius — defined as the half distance between neighbouring roots— and  $a$  the relative distance from  $r_0$  to  $r_m$  where water content equals bulk soil water content. In De Jong van Lier et al. (2013), this model is extended by taking into account the hydraulic resistances to water flow within the plant. Dividing water transport within the plant into two physical domains (from root surface to root xylem to leaf), assuming no water changes within the plant tissue and by coupling eq. 6 for water flow within the rhizosphere, they derived the following expression relating water potentials and  $T_a$ :

$$h_0(z) = h_l + \varphi(M_s(z) - M_0(z)) + \frac{T_a}{L_l} \quad (8)$$

where  $L_l$  ( $T^{-1}$ ) is the overall conductance over the root-to-leaf pathway and  $h_l$  (L) the leaf pressure head. Notice that  $S$  can be calculated by eq. 6 upon solving eq. 8.  $\varphi$  ( $T L^{-1}$ ) is defined as:

$$\varphi(z) = \frac{\rho r_m^2(z) \ln \frac{r_0}{r_x}}{2K_{root}} \quad (9)$$

where  $K_{root}$  ( $L T^{-1}$ ) is the radial root tissue conductivity (from root surface to root xylem) and  $r_x$  (L) the xylem radius.  $T_a$  is a function of  $h_l$ , which was defined piece-wisely by imposing a limiting value  $h_w$  on  $h_l$ :

$$T_r = \begin{cases} 1 & : h_l > h_w \\ 0 \leq T_r \leq 1 & : h_l = h_w \\ 0 & : h_l < h_w \end{cases} \quad (10)$$

where  $T_r (= T_a/T_p)$  is the relative crop transpiration. Crop water stress, a condition for which  $T_a < T_p$ , is defined at the crop level (Tardieu, 1996) and onsets when  $h_l = h_w$ . Because  $T_a$  and  $h_l$  are unknowns, eq. 8 and 10 cannot be solved analytically, but an efficient numerical algorithm is described in De Jong van Lier et al. (2013).

Fig. 2 helps to understand how RWU is distributed over depth.  $h_l$  can be regarded as a crop level measure of water deficit stress over the whole root zone: as soil gets drier,  $h_l$  is reduced, which increases the driving force for RWU (see RWU for the several values of  $h_l$  in Fig. 2). As soil pressure head  $h_s$  decreases, high uptakes are only achieved by lower  $h_l$ . For a certain  $h_l$  value, RWU is substantially reduced as  $h_s$  decreases. If  $h_l$  is not reduced as  $h_s$  gets lower,  $S$  becomes negative (negative  $S$  is not shown in Fig. 2, but it is part of an extension of each curve) and water will flow from root to soil. This situation occurs when parts of the root zone are wetter and RWU from these parts satisfies transpiration demand, and  $h_l$  is not reduced.

Fig. 2 also shows that RWU is sensitive to both  $R$  and  $h_s$ , and that it can be locally balanced by the  $R$  and soil water content. Under homogeneous soil water distribution, RWU is partitioned proportionally to  $R$ . For non-homogeneous conditions, RWU for lower  $R$  can be the same for higher  $R$  depending on the stress level (indicated by  $h_l$ ) and the  $h_s$  (see Fig. 2). This is in agreement with experimental results reported by several authors (Arya et al., 1975b, a; Green and Clothier, 1995; Verma et al., 2014) who found less densely-rooted but wetter parts of the root zone to correspond to a significant portion of RWU when more densely-rooted parts of the soil are drier, allowing the crop to maintain transpiration at potential rates. Due to empirical model concepts that employ only  $R$  for predicting RWU distribution over depth (for nonstressed conditions), these results have been interpreted as due to a mechanism labelled “compensation” by which uptake is “increased” from wetter layers to compensate



the “reduction” in the drier layers (Jarvis, 1989; Šimůnek and Hopmans, 2009). Clearly, this compensation concept is based on a reference RWU distribution based on  $R$  and is only relevant in empirical models. In physical models, discriminating compensation becomes less important since in such models “compensation” follows implicitly from the RWU mechanism.

In order to account for RWU pattern changes due to heterogeneous soil water distribution (the so-called “compensation”), several empirical models have been developed over the years. These models follow the general framework of the Feddes et al. (1978) model given by eq. 3. Below we review these models and present a new empirical alternative.

## 2.2 Empirical root water uptake models accounting for compensation

### 2.2.1 The Jarvis (1989) model

Jarvis (1989) defined a weighted-stress index  $\omega$  ( $0 \leq \omega \leq 1$ ) as

$$\omega = \int_{z_m} \alpha(z)\beta(z)dz. \quad (11)$$

where, differently from Feddes et al. (1978),  $\alpha$  was defined as a function of the effective saturation. In principle, any definition of  $\alpha$  is applicable in eq. 11, and in this paper we will refer to the Feddes et al. (1978) reduction function unless mentioned. Whereas Feddes et al. (1978) assume the RWU reduction directly to reflect in crop transpiration reduction, the Jarvis (1989) approach employs a so-called “whole-plant stress function” given by:

$$\frac{T_a}{T_p} = \min\left\{1, \frac{\omega}{\omega_c}\right\} \quad (12)$$

where  $\omega_c$  is a threshold value of  $\omega$  for the transpiration reduction. Substituting eq. 3 and 4 into eq. 1 (the continuity principle) and combining with eq. 12, results in:

$$S(z) = S_p\alpha(z)\alpha_2, \text{ where } \alpha_2 = \frac{1}{\max\{\omega, \omega_c\}} \quad (13)$$

where  $\alpha_2$  is called the compensation factor of RWU, distinct from the Feddes model (eq. 3) and which can be derived by defining  $T_a$  by eq. 12. In the Jarvis (1989) model,  $\alpha$  accounts for local reduction of RWU and transpiration reduction is computed by eq. 12. When  $\omega = 1$ , there is no RWU reduction ( $\alpha = 1$  throughout the root zone) and the model prediction is equal to the Feddes model. For  $\omega_c < \omega < 1$ , uptake is reduced in some parts of the root zone (as computed by  $\alpha < 1$ ) but the plant can still achieve potential transpiration rates by increasing RWU over the whole root zone by the factor  $\alpha_2$ . When  $\omega < \omega_c$ , the uptake is still increased by the factor  $\alpha_2$  but the potential transpiration rate cannot be met. The threshold value  $\omega_c$  places a limit on the plant’s ability to deal with soil water stress. When  $\omega_c$  tends to zero, eq. 12 tends to 1, and the plant can fully compensate uptake and transpire at the potential rate provided that  $\alpha > 0$  at some position within the root zone.

An analogy to stomata functioning is described by eq. 12 (Jarvis, 1989, 2011), putting this model in a more physical context. However, operational and physical limitations of this model have been raised (Skaggs et al., 2006; Javaux et al., 2013). The model introduces an additional parameter ( $\omega_c$ ), which should be determined by inverse modelling and is dependent on atmospheric demand, rooting properties (usually related to root length density) and soil type. Another difficulty is the conceptual



limitation raised by Skaggs et al. (2006), who showed that the model does not mimic compensation properly and affronts the definition of  $\alpha$ , as can be noticed by analysing eq. 13: RWU is reduced by  $\alpha$ , but increased by the factor  $1/\max[\omega, \omega_c]$ , making the interpretation of  $\alpha$  obscure. Another limitation is the linking of compensation to crop stress, making it to fail in predicting compensation under wet condition with a heterogeneous soil pressure head distribution (Javaux et al., 2013).

- 5 Using the piece-wise linear Feddes reduction function for  $\alpha$ , care must be taken in setting up and interpreting the threshold parameters of this function. The Feddes et al. (1978) model does not account for compensation, and the threshold pressure head value below which RWU is reduced ( $h_3$ ) also represents the value below which transpiration is reduced, making  $h_3$  values from literature usually to refer to this interpretation. Comparing to the Jarvis model, the transpiration reduction only takes place when  $\omega < \omega_c$ , and soil pressure head in some layers is already supposed to be more negative than  $h_3$ , which means
- 10 that  $h_3$  in Jarvis (1989) model is less negative than the equivalent in the Feddes model. In that sense,  $h_3$  for the Jarvis (1989) model is hard to determine experimentally. Inverse modelling by optimizing outcomes of soil water flow models with measured values of field experiments is an option.

### Comparison to the De Jong van Lier et al. (2008) model

The Jarvis (1989) model was shown to be “numerically” identical to De Jong van Lier et al. (2008) physical model, but only

15 under limiting hydraulic conditions (Jarvis, 2010, 2011). We briefly review this similarity and its implications on the empirical concept of the Jarvis (1989) model.

De Jong Van Lier et al. (2006) derived eq. 6 for describing RWU. Crop transpiration is obtained by integrating eq. 6 over  $z_m$  as defined in eq. 1, leaving two unknowns:  $M_0$  and  $T_a$ . In order to solve for these, De Jong van Lier et al. (2008) defined  $T_a$  as a piece-wise function as follows:

$$20 \quad \frac{T_a}{T_p} = \min \left\{ 1, \frac{T_{p_{\max}}}{T_p} \right\} \quad (14)$$

where  $T_{p_{\max}}$  ( $L T^{-1}$ ) is the maximum possible transpiration rate attained when  $M_0 = 0$ , given by:

$$T_{p_{\max}} = \int_{z_m} \rho(z) M(z) dz. \quad (15)$$

From eq. 14 when  $T_{p_{\max}} < T_p$ , drought stress occurs and  $T_a = T_{p_{\max}}$ . Under this condition, pressure head at the root surface reaches  $h_w \rightarrow M_0 = 0$  and  $S(z)$  becomes:

$$25 \quad S(z) = \rho(z) M(z). \quad (16)$$

When  $T_{p_{\max}} > T_p$ ,  $T_a = T_p$  (no drought stress) and  $M_0 (> 0)$  is given by:

$$M_0 = \frac{\int_{z_m} \rho(z) M(z) dz - T_p}{\int_{z_m} \rho(z) dz} \quad (17)$$





Jarvis (2011) observed the similarities between eq. [14] and [12] of the models. Notice also the algebraic similarity between  $\omega$  (eq. 11) and  $T_{p_{max}}$  (eq. 15). Thus, Jarvis (2010) showed that both models provide the same results for the stressed phase if  $\alpha$  and  $\beta(z)$  are defined as follows:

$$\alpha = \frac{M}{M_{max}} \quad (18)$$

5

$$\beta = \frac{\rho(z)}{\int_{z_m} \rho(z) dz} \quad (19)$$

where  $M_{max}$  is the maximum value of  $M$  (i.e., at  $h = 0$ ). By substituting eq. [18] and [19] into eq. 15 and comparing eq. 12 with eq. 14,  $\omega_c$  is found to be equal to:

$$\omega_c = \frac{T_p}{M_{max} \int_{z_m} \rho(z) dz} \quad (20)$$

10 Substitution of eq. [18] to [20] into eq. [12] and [11] results in eq. 16 of De Jong van Lier et al. (2008) model for stressed condition. Consequently, both models provide the same numerical results. For unstressed condition, analogous substitution results in:

$$S(z) = \rho(z)M(z) \frac{T_p}{T_{p_{max}}} = \frac{\rho(z)M(z)}{\int_{z_m} \rho(z)M(z) dz} T_p \quad (21)$$

Eq. 21 is different from eq. 6 and, therefore, the models cannot be correlated for these conditions. The Jarvis (1989) model 15 predicts RWU by a weighting factor between  $\rho$  and  $M$  throughout rooting depth. Defining  $\alpha$  and  $\beta$  by eq 18 and 19, respectively, allowed to correlate both models only for stressed conditions. These definitions and the resulting model will be further analysed.

### 2.2.2 The Li et al. (2001) model

Li et al. (2001) proposed to distribute potential transpiration over the root zone by a weighted stress index  $\zeta$ , being a function of both root distribution and soil water availability:

$$20 \quad \zeta(z) = \frac{\alpha(z)R(z)^\lambda}{\int_{z_m} \alpha(z)R(z)^\lambda dz} \quad (22)$$

where  $\alpha(-)$  and  $R$  ( $L L^{-3}$ ) were previously defined and the exponent  $\lambda$  is an empirical factor that modifies the shape of RWU distribution over depth. The smaller  $\lambda$ , the more water is taken up in deeper soil layers. Thus,  $S_p$  is given by:

$$S_p = \zeta(z)T_p \quad (23)$$





and RWU is calculated by substituting eq. 23 into eq. 3, following the Feddes approach.

Defining  $S_p$  as function of root length density and soil water availability distribution is an alternative to the Jarvis (2011) model. Compensation is directly accounted for by the weighted stress index in eq. 22. However, the choice of  $\alpha$  to represent soil water availability in eq. 22 does not mimic properly the compensation mechanism. Compensation may take place before transpiration reduction. Using  $\alpha$  in eq. 22 means that compensation will only take place after the onset of transpiration reduction when  $\alpha$  in one or more layers is less than unity. The  $\lambda$  parameter may also be interpreted as to account for compensation under non-stressed condition. Compensation, however, and shape of RWU distribution are likely to change as soil dries. A constant  $\lambda$  can not account for that.

### 2.2.3 The Molz and Remson (1970) and Selim and Iskandar (1978) models

Decades before Li et al. (2001), Molz and Remson (1970) and Selim and Iskandar (1978) had already suggested to distribute potential transpiration over depth according to root length density and soil water availability. Instead of using  $\alpha$  to account for soil water availability, they used soil hydraulic functions. The weighted stress index was defined as

$$\zeta(z) = \frac{\Gamma(z)R(z)}{\int_{z_m} \Gamma(z)R(z)dz} \quad (24)$$

where  $\Gamma$  is a soil hydraulic function to account for water availability. Molz and Remson (1970) used soil water diffusivity  $D$  ( $L^2T^{-1}$ ), and Selim and Iskandar (1978) used soil hydraulic conductivity  $K$  ( $LT^{-1}$ ) for  $\Gamma$  in eq. 24. RWU is then calculated by substituting eq. 24 into eq. 23 and then into eq. 3 following the Feddes approach.

These models may better represent RWU and compensation than the Li et al. (2001) model. The compensation is implicitly accounted for by means of  $\Gamma$  in  $\zeta$ . In drier soil layers,  $\Gamma$  is reduced, whereas in wetter soil layers  $\Gamma$  is increased, thus increasing RWU in these layers before the onset of transpiration reduction. Heinen (2014) compared different types of  $\Gamma$  in eq. 24 such as the relative hydraulic conductivity ( $K_r = K/K_{sat}$ ), relative matric flux potential ( $M_r = M/M_{max}$ ) and others. He found that using different forms of  $\Gamma$  provides very different patterns of RWU, but did not indicate a preference for a specific one.

### 2.2.4 Proposed empirical model

In describing soil water availability, the matric flux potential  $M$  may be a better choice than  $K$  or  $D$ , since it integrates  $K$  and  $h$  or  $D$  and  $\theta$  (Raats, 1974; De Jong van Lier et al., 2013). We propose a new weighted stress index, defined as:

$$\zeta_m(z) = \frac{R^\lambda M(h)}{\int_{z_m} R^\lambda M(h)dz} \quad (25)$$

The exponent  $\lambda$  provides additional flexibility on distribution of  $T_P$  over depth as was shown by Li et al. (2001).



### 3 Material and Methods

Table 1 summarizes the empirical RWU models evaluated in this study. They all follow the basic Feddes model (eq. 3), but diverging on how RWU is partitioned over rooting depth or how  $\alpha$  is defined. For each model, except for Jarvis (2010), we defined a modified version by substituting the Feddes reduction function by the proposed reduction function (Fig. 1b), and these modified versions were also evaluated. The threshold values of the Feddes et al. (1978) reduction function for anoxic conditions ( $h_1$  and  $h_2$ ) were set to zero. The value of the parameter  $h_4$  was set to  $-150$  m. The other parameters of the models were obtained by optimization as described in section 3.2.

All these models were embedded as sub-models into the ecohydrological model SWAP (Van Dam et al., 2008) in order to solve eq. 2 and to apply it for all kind of soil water flow conditions. Different scenarios of root length density, atmospheric demand and soil type (described in section 3.1) were set up in order to analyse the behaviour and sensitivity of the models. Simulation results of SWAP in combination with each of the RWU models were compared to the SWAP predictions when combined to the physical RWU model developed by De Jong van Lier et al. (2013).

The values of the De Jong van Lier et al. (2013) model parameters used in the simulations are listed in Table 2. The values of  $K_{root}$  and  $L_l$  are within the range reported by De Jong van Lier et al. (2013).

#### 3.1 Simulation scenarios

##### 3.1.1 Drying-out simulation

Boundary conditions for these simulations were no rain/irrigation and a constant atmospheric demand over time. The simulation continued until simulated crop transpiration by the physical RWU model approached zero. Soil evaporation was set to zero making the soil to dry out only due to RWU or drainage at the bottom. Free drainage (unit hydraulic gradient) at the maximum rooting depth was the bottom boundary condition. The soil was initially in hydrostatic equilibrium with a water table located at 1 m depth. We performed simulations for two levels of atmospheric demand given by potential transpiration  $T_p$ : 1 and 5 mm d<sup>-1</sup>. We also considered three types of soil and three levels of root length density, as described in the following.

##### 3.1.2 Soil type

Soil data for three top soils from the Dutch Staring series (Wösten et al., 1999) were used. The physical properties of these soils, described by the Mualem-van Genuchten functions (Mualem, 1976; Van Genuchten, 1980) for the  $K - \theta - h$  relations, are listed in Table 3. These soils are identified in this text as clay, loam and sand (Table 3).

##### 3.1.3 Root length density distribution

Three levels of root length density were used, according to the range of values normally found in the literature. We considered low, medium and high root length density for average crop values equal to 0.01, 0.1 and 1.0 cm cm<sup>-3</sup>, respectively. For all cases, we set the maximum rooting depth  $z_{max}$  equal to 0.5 m. Root length density over depth  $z$  was described by the



exponential function:

$$R(z_r) = R_0(1 - z_r) \exp^{-bz_r} \quad (26)$$

where  $R_0$  ( $L L^{-3}$ ) is the root length density at the soil surface,  $b$  (-) is a shape-factor parameter and  $z_r$  ( $= z/z_{max}$ ) is the relative soil root depth. The term  $(1 - z_r)$  in eq. 26 guarantees that root length density is zero at the maximum rooting depth.

- 5 The parameter  $R_0$  is hardly ever determined, whereas the average root length density of crops  $R_{avg}$  is usually reported in the literature. Assuming  $R$  of such a crop given by eq. 26, it can be shown that:

$$\int_0^1 R_0(1 - z_r) \exp^{-bz_r} dz_r = R_{avg} \quad (27)$$

Solving eq. 27 for  $R_0$  and substituting into eq. 26 gives:

$$R(z_r) = \frac{b^2 R_{avg}}{b + \exp^{-b} - 1} (1 - z_r) \exp^{-bz_r} \quad (b > 0) \quad (28)$$

- 10 Fig. 3 shows  $R(z_r)$  calculated from eq. 28 for different values of  $b$  and  $R_{avg} = 1 \text{ cm cm}^{-3}$ . As  $b$  approaches zero, eq. 28 tends to become linear, however it is not defined for  $b = 0$ . In our simulations  $b$  was arbitrarily set equal to 2.0.

### 3.2 Optimization

The parameters of the empirical RWU models were estimated by solving the following constrained optimization problem:

$$\text{minimize} \quad \Phi(\mathbf{p}) = \sum_{i=1}^n \sum_{j=1}^m [S_{i,j}^* - S_{i,j}(\mathbf{p})]^2 \quad (29)$$

subject to  $\mathbf{p} \in \Omega$

- 15 where  $\Phi(\mathbf{p})$  is the objective function to be optimized,  $S_{i,j}^*$  is the RWU simulated by SWAP model together with the De Jong van Lier et al. (2013) model at time  $i$  and depth  $j$  and  $S_{i,j}(\mathbf{p})$  is the corresponding RWU predicted by SWAP in combination with one of the empirical models shown in Table 1.  $\mathbf{p}$  is the model parameter vector to be optimized, constrained in the domain  $\Omega$ . Both  $\mathbf{p}$  and  $\Omega$  vary depending on the empirical RWU model used. Table 4 shows the parameters of each empirical RWU model that were optimized and their respective constraints  $\Omega$ .  $m$  and  $n$  are the number of soil layers and days of the simulation,  
 20 respectively. The Jarvis (2010) model has no empirical parameters and therefore requires no optimization.

- Eq. 29 was solved by using the PEST (Parameter ESTimation) tool (Doherty et al., 2005) coupled to the adapted version of SWAP. PEST is a non-linear parameter estimation program that solves eq. 29 by the Gauss-Levenberg-Marquardt (GLM) algorithm, searching for the deviation, initially along the steepest gradient of the objective function and switching gradually the search to Gauss-Newton algorithm as the minimum of the objective function is approached. Upon setting PEST parameters  
 25 we made reference runs of SWAP with each empirical model using random values of  $\mathbf{p}$  and assessed the ability of PEST for retrieving  $\mathbf{p}$ . These reference runs served to set up properly PEST for our case. For high non-linear problems as the one in eq. 29 GLM depends on the initial values of  $\mathbf{b}$ . We used five random sets of initial values for  $\mathbf{p}$  in order to guarantee that GLM found the global minimum and also to check the uniqueness of the solution.



The optimizations were performed for the drying-out simulation only. This guaranteed that RWU predictions from SWAP corresponded to the best fit of each empirical models to the De Jong van Lier et al. (2013) model. This analysis aimed to investigate the capacity of the empirical RWU models to mimic the RWU pattern predicted by the De Jong van Lier et al. (2013) model. These optimized parameters were subsequently used to evaluate the models in an independent growing season  
5 scenario.

### 3.2.1 Growing season simulation

The models were evaluated by simulating the transpiration of grass with weather data from the De Bilt weather station, the Netherlands (52°06' N; 5°11 'E), for the year 2006. The same root system distribution as in the drying-out simulations was used, i.e. a crop with roots exponentially distributed over depth as eq. 28 ( $b = 2.0$ ) down to 50 cm below soil surface. We also  
10 performed simulations for the same three types of soils and root length densities. In all cases the crop fully covered the soil with a leaf area index of 3.0. Daily reference evapotranspiration  $ET_0$  was calculated by SWAP using the FAO Penman-Monteith method (Allen et al., 1998). In SWAP model, a potential crop evapotranspiration  $ET_p$  is obtained by multiplying  $ET_0$  by a crop factor, which for the grass vegetation was set to 1 (Van Dam et al., 2008).  $ET_p$  was partitioned into potential evaporation  $E_p$  and  $T_p$  using parameter values for common crops given in SWAP model (see Van Dam et al. (2008) for details).

15 The values of the empirical parameters of each RWU model corresponding to the type of soil and root length density were taken from the optimizations performed in the drying-out experiment. Each parameter was estimated for two levels of  $T_p$  (1 and 5 mm d<sup>-1</sup>) and was linearly interpolated for intermediate levels of  $T_p$ . For  $T_p > 5$  mm d<sup>-1</sup> or  $T_p < 1$  mm d<sup>-1</sup>, the values estimated for these highest or lowest  $T_p$  values were used.

The bottom boundary condition was the same as in the drying-out simulations (free drainage). Initial pressure heads were  
20 obtained by iteratively running SWAP starting with the final pressure heads of the previous simulation until convergence.

## 4 Results and Discussion

### 4.1 Drying-out simulation

#### 4.1.1 Root water uptake pattern: De Jong van Lier et al. (2013) model

In this section we first focus on the behaviour of the De Jong van Lier et al. (2013) model in predicting RWU for the evaluated  
25 scenarios in the drying-out experiment. Fig. 4 shows the RWU patterns for the case of clay soil for the three evaluated root length densities  $R$  and the two levels of potential transpiration  $T_p$ . It can be seen how  $R$  and  $T_p$  affect RWU distribution and transpiration reduction as soil dries out. The onset and shape of transpiration reduction is affected by the RWU pattern. For low  $R$ , the low amount of roots in deeper layers is not sufficient to supply high RWU rates. When the upper layers become drier, transpiration reduction follows immediately. Under medium and high  $R$ , the RWU front moves gradually downward as water  
30 from the upper layers is depleted. For high  $R$ , the RWU front goes even deeper compared to medium  $R$ , and transpiration is sustained at potential rates for longer time (Fig. 4). Accordingly, the plant exploits the whole root zone and little water is left



when transpiration reduction onsets, causing an abrupt drop in transpiration. Regarding  $T_p$ , the RWU patterns are very similar for both evaluated rates, differing only in time scale: for high  $T_p$  the onset of transpiration reduction and the shift in RWU front occur earlier. The patterns for the sand and loam soil (not shown here) show very similar features.

The leaf pressure head  $h_l$  over time shown in Fig. 4 illustrates how the model adapts  $h_l$  to  $R$  and  $T_p$  levels and soil drying. Initially all scenarios have the same water content distribution and lower  $h_l$  values are required for low  $R$  or high  $T_p$  scenarios to supply potential transpiration rates. As soil becomes drier,  $h_l$  is decreased in order to increase the pressure head gradient between bulk soil and root surface and thus maintaining RWU corresponding to the potential demands. Therefore, uptake in wetter layers become more important. Transpiration reduction only onsets when  $h_l$  reaches the limiting leaf pressure head  $h_w$  ( $= -200$  m), after significant changes in the RWU patterns, characterized by increased uptake in deeper layers.

For the high  $T_p$ –low  $R$  scenarios, transpiration reduction starts at the first day of simulation although the soil is relatively wet. This is a case of transpiration reduction under non-limiting soil hydraulic conditions due to high atmospheric demand (Cowan, 1965). For such conditions, the high water flow within the plant required to attend the atmospheric demand cannot be supported by the root system with a low  $R$  and hydraulic parameters given in Table 2. Higher atmospheric demand (here represented by  $T_p$ ) increases the reduction of  $h_l$  caused by the hydraulic resistance to water flow within the plant, and the transpiration rate and RWU are a function of  $h_l$ . The physical model assumes a parsimonious relationship (eq. 10) between transpiration and  $h_l$ : transpiration rate is only reduced when  $h_l$  reaches a limiting value  $h_w$ , which corresponds to a maximum possible transpiration rate  $T_{p,max}$  allowed by the plant for the current soil hydraulic and atmospheric conditions. Under non-limiting soil hydraulic conditions,  $T_{p,max}$  is a function of root system properties and plant hydraulic parameters only (Table 2). Fig. 5 shows  $T_{p,max}$  as a function of  $K_{root}$  for some values of  $L_l$  with a constant soil pressure head in the root zone of -1 m for the low  $R$  in the sandy soil. It can be seen that  $K_{root}$  is limiting the crop transpiration and that  $L_l$  becomes important only when  $K_{root}$  increases. The potential transpiration can be achieved by raising  $K_{root}$  up to about  $10^{-7}$  m d $^{-1}$ . This can also be achieved by decreasing  $h_w$  (not shown in Fig. 5).

In the field, transpiration rate and root length density are related to each other: a high transpiration rate only occurs at high leaf area and a high leaf area implies a high root length density. Thus, even in very dry and hot weather conditions, a crop with a low  $R$  may not be able to realize high transpiration. Furthermore, crop transpiration depends on the stomatal conductance. In the De Jong van Lier et al. (2013) model, this is implicitly taken into account by the simple relationship between  $h_l$  and  $T_a$ . However, stomatal conductance is relatively complex and depends on several environmental factors such as air temperature, solar radiation and CO $_2$  concentration. Thus, high potential transpiration rate may not be achieved because of the stomatal conductance reduction due to temperature or solar radiation. These results can be enhanced by the coupling of the De Jong van Lier et al. (2013) model to stomatal conductance models, such as the Tuzet et al. (2003) model.

#### 4.1.2 Root water uptake pattern predicted by the empirical models

In this section, we evaluate the empirical RWU models (models and their abbreviations are listed in Table 1) based on the comparison of RWU patterns and transpiration reduction over time with the respective predictions from the De Jong van Lier



et al. (2013) model (VLM). All empirical model predictions are performed with respective optimized parameters as shown in Table 5 and are discussed in section 4.1.4, thus representing the best fit with VLM.

The RWU patterns simulated by VLM and the empirical models for the scenario of sandy soil and high  $R$  are shown in Fig. 6 and 7 for low and high  $T_p$ , respectively. Both versions of Feddes model (FM and FMm) predicted enhanced RWU from the upper soil layers. When the pressure head ( $h_s$ ) (for FM) or soil matric flux potential ( $M_s$ ) (for FMm) is greater than the threshold value for uptake reduction, these uptake patterns are equivalent to the vertical  $R$  distribution. For conditions drier than the threshold value (when  $\alpha_f$  and  $\alpha_m$  are less than 1), the predicted RWU patterns by the models become different (Fig. 6 and 7).

After a period of reduced RWU, the length of which depends on  $R$ ,  $T_p$  and  $h_3$ , RWU from the upper soil layers predicted by FM rapidly decreases to zero. This zero-uptake zone expands downward as soil dries out. On the other hand, the uptake predicted by FMm is substantially reduced right after the onset of transpiration reduction, proceeding at lower rates and a much longer time until approaching zero. These features become evident by comparing the shape of both reduction functions (Fig. 8).  $\alpha_m$  is linear with  $M$  after  $M > M_c$ , but it is concavely-shaped as a function of  $h$  — as also shown by Metselaar and De Jong van Lier (2007) and De Jong van Lier et al. (2009). Thus,  $\alpha_m$  is abruptly reduced for  $M > M_c$ , causing substantial reduction in RWU even when  $h$  is slightly below the threshold value. Therefore, RWU proceeds at low rates for longer time. Conversely, due to the linear shape of  $\alpha_f$ , RWU predicted by FM remains higher for a longer time after  $h < h_3$ . No abrupt change in RWU patterns is predicted by this model, especially when  $T_p$  is low (Fig. 6). When  $h$  comes close to  $h_4$ ,  $\alpha_f$  is still relatively high and RWU continues, making  $h$  to rapidly approach  $h_4$ . Another diverging feature between  $\alpha_f$  and  $\alpha_m$ , also shown in Fig. 8, is that the shape of  $\alpha_m$  varies with soil type (regardless the value of its threshold parameter  $M_c$ ), whereas  $\alpha_f$  does not. These different features of the reduction functions also affect the matching values of the parameters as discussed below. The choice of the reduction function, however, affects transpiration curve over time only slightly, but RWU patterns are strongly affected (Fig. 6 and 7).

The RWU patterns predicted by JM and JMm models can be very different, as shown by Fig. 6 for the high  $R$ –low  $T_p$  scenario. In fact, the JM model did not predict any compensation at all because the optimal  $\omega_c$  was equal to unity (Table 5) — thus becoming identical to FM — and the optimal  $h_3$  for JM and FM were similar. These high  $R$ –low  $T_p$  scenarios with a high  $R$  in deep soil layers allow RWU at higher rates when surface soil layers becomes drier (as predicted by VLM). Then, reducing  $\omega_c$  in an attempt to predict compensation with JM makes RWU pattern to deviate even more from the VLM pattern. This is illustrated in Fig. 6 and by the optimal  $h_3$  and  $\omega_c$  values shown in Table 5. In order to mimic the VLM uptake patterns, the value of  $h_3$  for all soil types in this scenario was equal or close to zero. Decreasing  $h_3$  or  $\omega_c$  in order to simulate compensation makes JM predicting higher uptake from upper layers, increasing the discrepancy between the models. The optimal  $\omega_c$  for all soil types was equal to 1 (in other words: no compensation). RWU in the upper layers predicted by VLM is substantially reduced within a few days, whereas reducing  $\omega_c$  in JM model to predict compensation causes also an increase of uptake in upper layers. The model, therefore, cannot mimic the scenarios with compensation evaluated here. Conversely, the JMm was able to reproduce considerably well the VLM pattern for these scenarios due to the shape of  $\alpha_m$  as discussed above. As soon



as  $M > M_c$  in the upper layers, RWU decreased at a higher rate, compensated by increasing uptake from the wetter, deeper layers. This agrees more closely to VLM predictions.

For high  $T_p$  (Fig. 7), the JM model can predict compensation ( $\omega_c < 1$ ), however its predicted RWU pattern is very different from JMm and VLM. JM predicts a higher RWU near the soil surface for a longer period than the other models that account for compensation. This makes soil water depletion to be more intense and RWU from these layers will cease sooner when  $h_s$  becomes lower than  $h_4$ . At this point,  $T_a$  is predicted to continue equal to  $T_p$  because of the low optimal  $\omega_c$  ( $= 0.19$ ), which increases RWU from the deeper layers where  $h > h_4$ . JMm behaved very differently with uptake over the first few days (when  $M_s > M_c$ ) in accordance with  $R$  distribution. After  $M < M_c$  in upper soil layers, the RWU pattern started to change gradually and RWU increased at lower depths.

The proposed models (PM and PMm) are capable of predicting similar RWU patterns as VLM. For the low  $T_p$ -high  $R$  scenario (Fig. 6), RWU is more uniformly distributed over depth than in the VLM model for the first days and uptake from upper layers is lower than that predicted by VLM model. For high  $T_p$  (Fig. 7), these models better represent RWU patterns and, in general, there is not much difference in predictions of RWU between the proposed models. The shape of the transpiration reduction over time however, is smoother than the VLM model. Concerning the relative transpiration curve, the proposed models appear to be less precise than the other models that account for RWU compensation.

JMII does not mimic well the RWU pattern for the high  $R$ -low  $T_p$  scenarios. It overestimates uptake from surface layers for the first days. Before the onset of transpiration reduction, uptake from upper layers becomes zero, but is compensated by a higher uptake from deeper layers. The model is very sensitive to either  $R$  or  $M$ . For the high  $R$ -high  $T_p$  scenarios JMII provides better uptake pattern predictions (Fig. 7). However, the model does not perform well in the other scenarios of low and medium  $R$  (data not shown here), which will be discussed in section 4.1.3.

### 4.1.3 Statistical indices

The performance of the empirical models was analysed by the coefficient of determination  $r^2$  and the model efficiency coefficient  $E$  (Nash and Sutcliffe, 1970) calculated by comparing to the RWU and relative transpiration predicted by VLM. For the low  $R$ -high  $T_p$  scenarios, the VLM predicts water stress ( $T_a < T_p$ ) since the beginning of the simulation as discussed in section 4.1.1. The empirical models (except for JM and JMm by setting  $\omega_c > 1$ ) are not able to reproduce these results, thus these scenarios are not taken into account on analysing the performance of the models.

These statistical indices for the evaluated scenarios of each model are concisely shown by the boxplots in Fig. 9. The width of whiskers indicates the range of the statistical indices for each model used in the evaluated scenarios. The outliers indicate whether a model had different performance at some scenarios than its overall performance. Focusing first on RWU, it can be easily seen the better performance of the proposed models. The performance of PM was just a bit poorer than PMm's, showed by the presence of an outlier and lower median. JMm performed as good as the proposed models, and only in two scenarios it had bad performance as shown by the outliers in Fig. 9. The wider whiskers and presence of outliers of the other models confirm their poorer performances.





Among the models that account for RWU compensation, JM and JMII had the poorest performances. These models had very low performances in the high  $R$ –low  $T_p$  scenarios and in general their performances were poorer for medium  $R$  scenarios, especially for low  $T_p$ . Thus, the use of  $\alpha_m$  to replace Feddes original reduction function  $\alpha_f$  in Jarvis (1989) model promotes substantial improvements, especially from medium to high  $R$  scenarios. For low  $R$  scenarios all models performed well and the highest values of the boxes in Fig. 9 usually refer to this scenario.

On predicting transpiration all models accounting for compensation performed well, except JM. It can be noticed that JMII performed much better on predicting transpiration than RWU. Similarly as for the RWU predictions, all models had their poorest performance in the high  $R$  scenarios.

#### 4.1.4 Relation of the optimal empirical parameters to $R$ and $T_p$ levels

The optimal values of the empirical parameters of all models (except for JMII that has no empirical parameters) for all scenarios (except for the high  $T_p$ –low  $R$  scenario) are shown in Table 5. The threshold reduction transpiration parameters  $h_3$  and  $M_c$  (for FM and FMm, respectively) stands for the soil hydraulic conditions from which the crop cannot meet its potential transpiration rate. Conceptually, the more the roots, the lower is  $h_3$  or  $M_c$  due to the larger root surface area for RWU, i.e. the crop can extract water in drier soil conditions. Similarly, lower  $h_3$  and  $M_c$  are expected for low  $T_p$ . This can also be deduced from Fig. 6 and 7 by means of the predictions of relative transpiration and RWU by VLM.

The optimal  $h_3$  and  $M_c$  values (Table 5) for FM and FMm, respectively, increase as  $R$  or  $T_p$  increases, contradicting their conceptual relation to  $R$  and  $T_p$  levels. In drying-out scenarios, soil water from top layers depletes rapidly due to the higher initial uptake. As a result, uptake from these layer starts to decrease whereas RWU in deeper, wetter layers increases. The higher the  $R$ , the more intense is this process as seen by the VLM predictions in section 4.1.1. Because FM and FMm do not account for this mechanism, decreasing  $h_3$  or  $M_c$  in search for conceptually meaningful values would make these models to predict higher RWU at upper layers (in accordance with  $R$  distribution) for a longer period, increasing the discrepancy with VLM predictions. Therefore, their best fitted values are physically without meaning due to the model assumptions.

In order to interpret the parameters in Table 5 for JM, one should first recall that  $\alpha$  in JM stands for the local RWU reduction due to soil resistance. Thus, its  $h_3$  parameter refers the local soil pressure at which RWU starts to reduce. It may be argued that RWU reduction occurs in drier soil conditions as  $R$  increases, that is  $h_3$  is more negative for higher  $R$  (similarly as for FM and FMm). However, since JM accounts for compensation, RWU is interpreted as a non-local process, i.e. uptake in one layer depends on water status and root properties from other layers (Javaux et al., 2013). Thus, JM's  $h_3$  parameter is affected by other parts of the root zone. Predictions by VLM show that RWU reduction from the upper layers starts at less negative soil pressure head as  $R$  increases. Therefore,  $h_3$  in JM should increase as  $R$  increases. The values of  $h_3$  for JM shown in Table 5 agrees to this conceptual meaning. The JMm's  $M_c$  parameter can be interpreted likewise.

The JM's  $\omega_c$  parameter values for the high  $R$ –low  $T_p$  scenarios equal 1, thus contradicting its conceptual meaning: as in these scenarios the compensation mechanism is more intense,  $\omega_c$  should be less than one for the medium and high  $R$  scenarios. The reason for  $\omega_c = 1$  was discussed in section 4.1.2. Conversely,  $\omega_c$  values for JMm follow the conceptual meaning.



The optimal parameters of the proposed models follow the logical relation to  $R$  and  $T_p$ . The  $l$  values for both models are very close. The optimal  $l$  values are less sensitive to soil types and more sensitive to  $R$ .

## 4.2 Growing season simulation

By evaluating the RWU models under real weather conditions during a relatively dry year and considering the same soil types and crop characteristics as for the drying-out experiment, it was possible to use the respective soil type and root length density specific calibrated parameters. We did not evaluate the models for the low  $R$  scenario because the empirical models (except JM and JMm) were not able to mimic those conditions for high  $T_p$  (section 4.1.1). This evaluation is also important to analyse whether calibration of an empirical model with a single drying-out experiment type results in consistent behaviour in other circumstances.

Table 6 shows the cumulative actual transpiration simulated by SWAP using all the RWU models. Actual cumulative transpiration predicted by VLM for low  $R$  was much lower and approximately equal for the three soil types (40.45, 40.05 and 40.08 cm for clay, loam and sand soil, respectively). In fact, a higher  $R$  resulted in an increasing difference of cumulative transpiration between soil types. Most water is extracted from the clay soil, followed by sand and loam. Little difference of cumulative transpiration is found between medium and high  $R$ : for sand and clay soil, the cumulative transpiration was slightly higher for high  $R$  and practically identical for the loam soil.

Comparing cumulative  $T_a$  predicted by the empirical models with VLM predictions shows that the models that do not account for compensation underestimate cumulative  $T_a$  from 2.0 % (medium  $R$ –sand soil scenario) to 13.9 % (high  $R$ –clay soil scenario). Overall, the highest underestimates occurred for high  $R$ . All other models predict similar values. Therefore, for total actual transpiration any of the evaluated models accounting for compensation might be suitable after calibration.

An overall analysis of the models performance is shown in Fig. 10. The best performances are from the models that account for compensation. An improvement of JM by using the proposed reduction function can be observed. Among the models that account for compensation, JM had the worst performance. JMII also was poor in predicting RWU. Overall, the best performances were also obtained by the proposed models (PM and PMm) and by the modified Jarvis (1989) model (JMm). These results also indicate that the strategy to calibrate an empirical model in a single drying-out experiment is successful.

## 5 Conclusions

Several simple RWU models have been developed over the years and here we outlined some of these models and also proposed alternatives. Some of these models were embedded as sub-models into the eco-hydrological model SWAP (Van Dam et al., 2008) and their evaluation was based on the comparison of RWU predictions performed by the physical De Jong van Lier et al. (2013) model (also embedded into the SWAP model) for two numerical experiments with several scenarios of soil type, root length density and potential transpiration. The parameters of the empirical models were determined by inverse modelling of simulated RWU. The simulated scenarios allowed insight into the behaviour of the De Jong van Lier et al. (2013) model, especially under wet soil conditions and high potential transpiration. We found that for the low  $R$ –high  $T_p$  scenarios the De



Jong van Lier et al. (2013) model predicts crop transpiration reduction in wet soil conditions. For such cases, the maximum crop transpiration rate is dependent on crop hydraulic parameters, especially the radial root hydraulic conductivity. More insight into these results may be obtained by coupling the De Jong van Lier et al. (2013) physical model with stomatal conductance models. Regarding the performance of the empirical models we conclude:

- 5     • The widely-used Feddes et al. (1978) empirical RWU model performs well only under circumstances of low root length density  $R$ , that is for the scenarios of low root water “compensation”. From medium to high  $R$ , the model cannot mimic properly the RWU dynamics as predicted by the De Jong van Lier et al. (2013) model, resulting in very poor predictions. Besides, the optimized  $h_3$  values are counterintuitive when interpreting their conceptual meaning. Using our proposed RWU reduction function (the FMm model) does not improve performance either.
- 10    • The Jarvis (1989) model provides good predictions only for low and medium  $R$  scenarios. For high  $R$ , the model cannot mimic the RWU patterns predicted by the De Jong van Lier et al. (2013) model. Using our proposed reduction function (the JMm model) helps to improve RWU predictions. Similarly, the JMII model does not perform well for high  $R$ –low  $T_p$  scenarios.
  - The proposed models are capable of predicting RWU patterns similar to those obtained by the De Jong van Lier et al. (2013) model. The statistical indices point them as the best alternatives to mimic RWU predictions by the De Jong van Lier
- 15    et al. (2013) model.
  - The simulations for a growing season experiment confirmed these findings, suggesting that a single experiment of soil drying-out is sufficient to analyse the performance of RWU models and retrieve their empirical parameters by defining the objective function in terms of RWU.

*Acknowledgements.* The first author wishes to thank CAPES (The Capes Foundation, Ministry of Education of Brazil) and CNPq (National  
20 Counsel of Technological and Scientific Development, Brazil) for the PhD scholarship.



## References

- Allen, R. G., Pereira, L. S., Raes, D., Smith, M., et al.: Crop evapotranspiration-Guidelines for computing crop water requirements-FAO Irrigation and drainage paper 56, FAO, Rome, 300, 1998.
- Arya, L. M., Blake, G. R., , and Farrell, D. A.: A field study of soil water depletion patterns in presence of growing soybean roots: III. Rooting characteristics and root extraction of soil water, *Soil Science Society of America Journal*, 39, 437–444, 1975a.
- 5 Arya, L. M., Blake, G. R., and Farrell, D. A.: A field study of soil water depletion patterns in presence of growing soybean roots: II. Effect of plant growth on soil water pressure and water loss patterns, *Soil Science Society of America Journal*, 39, 430–436, 1975b.
- Braud, I., Varado, N., and Olioso, A.: Comparison of root water uptake modules using either the surface energy balance or potential transpiration, *Journal of Hydrology*, 301, 267–286, 2005.
- 10 Brooks, R. H. and Corey, A. J.: Hydraulic properties of porous media, *Hydrol. Paper*, 1964.
- Casaroli, D., De Jong Van Lier, Q., and Dourado, Neto, D.: Validation of a root water uptake model to estimate transpiration constraints, *Agricultural Water Management*, 97, 1382–1388, 2010.
- Chahine, M. T.: The hydrological cycle and its influence on climate, *Nature*, 359, 373–380, 1992.
- Cowan, I. R.: Transport of water in the soil-plant-atmosphere system, *Journal of Applied Ecology*, pp. 221–239, 1965.
- 15 De Jong Van Lier, Q., Metselaar, K., and Van Dam, J. C.: Root water extraction and limiting soil hydraulic conditions estimated by numerical simulation, *Vadose Zone Journal*, 5, 1264–1277, 2006.
- De Jong van Lier, Q., Van Dam, J. C., Metselaar, K., De Jong, R., and Duijnsveld, W. H. M.: Macroscopic root water uptake distribution using a matric flux potential approach, *Vadose Zone Journal*, 7, 1065–1078, 2008.
- De Jong van Lier, Q., Dourado, Neto, D., and Metselaar, K.: Modeling of transpiration reduction in van Genuchten–Mualem type soils, *Water Resources Research*, 45, W02 422, 2009.
- 20 De Jong van Lier, Q., van Dam, J. C., Durigon, A., Santos, M. A., and Metselaar, K.: Modeling water potentials and flows in the soil-plant system comparing hydraulic resistances and transpiration reduction functions, *Vadose Zone Journal*, in press, 2013.
- De Willigen, P. and van Noordwijk, M.: Roots, plant production and nutrient use efficiency, Ph.D. thesis, Wageningen Agric. Univ., The Netherlands, 1987.
- 25 de Willigen, P., van Dam, J. C., Javaux, M., and Heinen, M.: Root water uptake as simulated by three soil water flow models, *Vadose Zone Journal*, 11, 2012.
- Denmead, O. T. and Shaw, R. H.: Availability of soil water to plants as affected by soil moisture content and meteorological conditions, *Agronomy Journal*, 54, 385–390, 1962.
- Doherty, J., Brebber, L., and Whyte, P.: PEST: Model-independent parameter estimation, Watermark Computing, Corinda, Australia, 122, 30 2005.
- Dong, X., Patton, B. D., Nyren, A. C., Nyren, P. E., and Prunty, L. D.: Quantifying root water extraction by rangeland plants through soil water modeling, *Plant and soil*, 335, 181–198, 2010.
- Doorenbos, J. and Kassam, A.: Yield response to water., FAO Irrig. Drain. Pap. 33., FAO, Rome., 1986.
- Feddes, R., Kowalik, P., Kolinska-Malinka, K., and Zaradny, H.: Simulation of field water uptake by plants using a soil water dependent root extraction function, *Journal of Hydrology*, 31, 13–26, 1976.
- 35 Feddes, R., Kowalik, P., and Zaradny, H.: Simulation of field water use and crop yield., Simulation Monograph Series. Pudoc, Wageningen, The Netherlands., 1978.



- Feddes, R. A. and Raats, P. A. C.: Parameterizing the soil–water–plant root system, in: *Unsaturated-zone modeling: Progress, challenges, and applications*, edited by Feddes, R. A., ROOIJ, G. H., and VAN, DAM, J. C., pp. 95–141, Wageningen UR Frontis Series. Kluwer Academic Publ., Dordrecht, The Netherlands, 2004.
- Fisher, M. J., Charles-Edwards, D. A., and Ludlow, M. M.: An analysis of the effects of repeated short-term soil water deficits on stomatal conductance to carbon dioxide and leaf photosynthesis by the legume *Macroptilium atropurpureum* cv. Siratro, *Functional Plant Biology*, 8, 347–357, 1981.
- Gardner, W. R.: Dynamic aspects of water availability to plants, *Soil Science*, 89, 63, 1960.
- Green, S. and Clothier, B.: The root zone dynamics of water uptake by a mature apple tree, *Plant and Soil*, 206, 61–77, 1999.
- Green, S. R. and Clothier, B. E.: Root water uptake by kiwifruit vines following partial wetting of the root zone, *Plant and soil*, 173, 317–328, 1995.
- Heinen, M.: FUSSIM2: brief description of the simulation model and application to fertigation scenarios, *Agronomie*, 21, 285–296, 2001.
- Heinen, M.: Compensation in Root Water Uptake Models Combined with Three-Dimensional Root Length Density Distribution, *Vadose Zone Journal*, 13, 2014.
- Jarvis, N.: Comment on “Macroscopic root water uptake distribution using a matric flux potential approach”, *Vadose Zone Journal*, 9, 499–502, 2010.
- Jarvis, N.: Simple physics-based models of compensatory plant water uptake: concepts and eco-hydrological consequences, *Hydrology and Earth System Sciences Discussions*, 8, 6789–6831, 2011.
- Jarvis, N. J.: A simple empirical model of root water uptake, *Journal of Hydrology*, 107, 57–72, 1989.
- Javaux, M., Schröder, T., Vanderborght, J., and Vereecken, H.: Use of a three-dimensional detailed modeling approach for predicting root water uptake, *Vadose Zone Journal*, 7, 1079–1088, 2008.
- Javaux, M., Couvreur, V., Vanderborght, J., and Vereecken, H.: Root water uptake: From three-dimensional biophysical processes to macroscopic modeling approaches, *Vadose Zone Journal*, 12, 2013.
- Lai, C. T. and Katul, G.: The dynamic role of root-water uptake in coupling potential to actual transpiration, *Advances in Water Resources*, 23, 427–439, 2000.
- Li, K. Y., De, Jong, R., and Boisvert, J. B.: An exponential root-water-uptake model with water stress compensation, *Journal of Hydrology*, 252, 189–204, 2001.
- Li, K. Y., De, Jong, R., Coe, M. T., and Ramankutty, N.: Root-water-uptake based upon a new water stress reduction and an asymptotic root distribution function, *Earth Interactions*, 10, 1–22, 2006.
- Li, Y., Fuchs, M., Cohen, S., Cohen, Y., and Wallach, R.: Water uptake profile response of corn to soil moisture depletion, *Plant, Cell & Environment*, 25, 491–500, 2002.
- Metselaar, K. and De Jong van Lier, Q.: The shape of the transpiration reduction function under plant water stress, *Vadose Zone Journal*, 6, 124–139, 2007.
- Molz, F. and Remson, I.: Extraction term models of soil moisture use by transpiring plants, *Water Resources Research*, 6, 1346–1356, 1970.
- Molz, F. J.: Models of water transport in the soil-plant system, *Water Resour. Res.*, 17, 1245–1260, 1981.
- Mualem, Y.: A new model for predicting the hydraulic conductivity of unsaturated porous media, *Water resources research*, 12, 513–522, 1976.
- Nash, J. and Sutcliffe, J.: River flow forecasting through conceptual models part I—A discussion of principles, *Journal of hydrology*, 10, 282–290, 1970.



- Passioura, J.: Water transport in and to roots, *Annual Review of Plant Physiology and Plant Molecular Biology*, 39, 245–265, 1988.
- Prasad, R.: A linear root water uptake model, *Journal of Hydrology*, 99, 297–306, 1988.
- Raats, P.: Steady flows of water and salt in uniform soil profiles with plant roots, *Soil Science Society of America Journal*, 38, 717–722, 1974.
- 5 Raats, P. A. C.: Uptake of water from soils by plant roots, *Transport in porous media*, 68, 5–28, 2007.
- Selim, H. and Iskandar, I.: Nitrogen behavior in land treatment of wastewater: A simplified model, *State of Knowledge in Land Treatment of Wastewater*, 1, 171–179, 1978.
- Šimůnek, J. and Hopmans, J. W.: Modeling compensated root water and nutrient uptake, *Ecological modelling*, 220, 505–521, 2009.
- Skaggs, T. H., Van Genuchten, M. T., Shouse, P. J., and Poss, J. A.: Macroscopic approaches to root water uptake as a function of water and
- 10 salinity stress, *agricultural water management*, 86, 140–149, 2006.
- Tardieu, F.: Drought perception by plants Do cells of droughted plants experience water stress?, *Plant growth regulation*, 20, 93–104, 1996.
- Taylor, H. and Klepper, B.: The role of rooting characteristics in the supply of water to plants, *Adv. Agron*, 30, 99–128, 1978.
- Taylor, S. and Ashcroft, G.: *Physical Edaphology*, 1972.
- Tuzet, A., Perrier, A., and Leuning, R.: A coupled model of stomatal conductance, photosynthesis and transpiration, *Plant, Cell & Environ-*
- 15 *ment*, 26, 1097–1116, 2003.
- Van Dam, J. C., Groenendijk, P., Hendriks, R. F. A., and Kroes, J. G.: Advances of modeling water flow in variably saturated soils with SWAP, *Vadose Zone Journal*, 7, 640–653, 2008.
- Van Genuchten, M. T.: A closed-form equation for predicting the hydraulic conductivity of unsaturated soils, *Soil Science Society of America Journal*, 44, 892–898, 1980.
- 20 Vandoorne, B., Beff, L., Lutts, S., and Javaux, M.: Root Water Uptake Dynamics of var. Under Water-Limited Conditions, *Vadose Zone Journal*, 11, 2012.
- Verma, P., Loheide, S. P., Eamus, D., and Daly, E.: Root water compensation sustains transpiration rates in an Australian woodland, *Advances in Water Resources*, 74, 91–101, 2014.
- Vrugt, J., Wijk, M. v., Hopmans, J. W., and Šimunek, J.: One-, two-, and three-dimensional root water uptake functions for transient modeling,
- 25 *Water Resources Research*, 37, 2457–2470, 2001.
- Wösten, J., Lilly, A., Nemes, A., and Le Bas, C.: Development and use of a database of hydraulic properties of European soils, *Geoderma*, 90, 169–185, 1999.
- Yadav, B. K., Mathur, S., and Siebel, M. A.: Soil moisture dynamics modeling considering the root compensation mechanism for water uptake by plants, *Journal of Hydrologic Engineering*, 14, 913–922, 2009.
- 30 Yu, G. R., Zhuang, J., Nakayama, K., and Jin, Y.: Root water uptake and profile soil water as affected by vertical root distribution, *Plant Ecology*, 189, 15–30, 2007.
- Zur, B., Jones, J., Boote, K., and Hammond, L.: Total resistance to water flow in field soybeans: II. Limiting soil moisture, *Agronomy Journal*, 74, 99–105, 1982.



## List of tables

**Table 1.** Summary of empirical models used.  $\alpha_f$  and  $\alpha_m$  are the Feddes et al. (1978) (Fig. 1a) and proposed reduction functions (Fig. 1b),  $S_p$  (eq. 4) is the potential root water uptake,  $\omega$  (eq. 11) and  $\omega_c$  are the weighted stress index and threshold value in Jarvis (1989) model and  $\zeta_m$  (eq. 25) is the weighted stress index in the proposed models.

Model	Acronym	Equation
Feddes et al. (1978) model	FM	$S(z) = S_p \alpha_f$
Modified Feddes et al. (1978) model	FMm	$S(z) = S_p \alpha_m$
Jarvis (1989) model	JM	$S(z) = S_p \frac{\alpha_f}{\max\{\omega, \omega_c\}}$
Modified Jarvis (1989) model	JMm	$S(z) = S_p \frac{\alpha_m}{\max\{\omega, \omega_c\}}$
Jarvis (2010) model	JMII	Eqs. 11 to 13 with parameters given by eqs. 18 to 20
proposed model I	PM	$S(z) = \zeta_m T_p \alpha_f$
proposed model II	PMm	$S(z) = \zeta_m T_p \alpha_m$





**Table 2.** Values of the parameters of De Jong van Lier et al. (2013) model used in the simulations.

Parameter	Value	Unit
$r_0$	0.5	mm
$r_x$	0.2	mm
$K_{root}$	$3.5 \cdot 10^{-8}$	$\text{m d}^{-1}$
$L_l$	$1 \cdot 10^{-6}$	$\text{d}^{-1}$
$h_w$	-200	m



**Table 3.** Mualem-van Genuchten parameters for three soils of the Dutch Staring series (Wösten et al., 1999) used in simulations.  $\theta_s$  and  $\theta_r$  are the saturated and residual water content, respectively;  $K_s$  is saturated hydraulic conductivity and  $\alpha$ ,  $\lambda$  and  $n$  are fitting parameters.

Staring soil ID	Textural class	Reference in this paper	$\theta_r$	$\theta_r$	$K_s$	$\alpha$	$\lambda$	$n$
			$\text{m m}^{-3}$	$\text{m m}^{-3}$	$\text{m d}^{-1}$	$\text{m}^{-1}$	-	-
B3	Loamy sand	Sand	0.02	0.46	0.1542	1.44	-0.215	1.534
B11	Heavy Clay	Clay	0.01	0.59	0.0453	1.95	-5.901	1.109
B13	Sand Loam	Loam	0.01	0.42	0.1298	0.84	-1.497	1.441

**Table 4.** Parameters of the root water uptake models estimated by optimization and their respective constraints  $\Omega$ .

Model	Parameter	$\Omega$	Unit
FM	$h_3$	$-150 < h_3 < 0$	m
FMm	$M_c$	$0 < M_c < M_{max}$	$\text{m}^2 \text{d}^{-1}$
JM	$h_3$	$-150 < h_3 < 0$	m
	$\omega_c$	$0 < \omega_c \leq 1$	-
JMm	$M_c$	$0 < M_c < M_{max}$	$\text{m}^2 \text{d}^{-1}$
	$\omega_c$	$0 < \omega_c \leq 1$	-
PM	$h_3$	$-150 < h_3 < 0$	m
	$l_m$	$0 < l_m \leq 1$	-
PMm	$M_c$	$0 < M_c < M_{max}$	$\text{m}^2 \text{d}^{-1}$
	$l_m$	$0 < l_m \leq 1$	-



**Table 5.** Optimal parameters of each empirical model for all scenarios in the drying-out experiment

Soil	Tp	RD	FM	FMm	JM	JMm		PM		PMm		
			$h_3$	$M_c$	$h_3$	$\omega_c$	$M_c$	$\omega_c$	$h_3$	$l$	$M_c$	$l$
	mm d <sup>-1</sup>	cm cm <sup>-3</sup>	cm	cm <sup>2</sup> d <sup>-1</sup>	cm	-	cm <sup>2</sup> d <sup>-1</sup>	-	cm	-	cm <sup>2</sup> d <sup>-1</sup>	-
clay	1	0.01	-1968.7	0.213	-284.5	0.711	0.366	0.494	-1615.7	1.322	0.227	1.290
clay	1	0.10	-1211.0	0.329	-132.4	0.196	0.944	0.024	-7579.9	0.869	0.076	0.884
clay	1	1.00	-1.7	0.950	-0.0	1.000	5.971	0.004	-10673.7	0.354	0.022	0.342
loam	1	0.01	-7588.1	0.334	-5.0	0.457	22.483	0.016	-6927.6	1.086	0.408	1.084
loam	1	0.10	-6085.6	0.487	-93.9	0.126	25.721	0.002	-11795.6	0.911	0.113	0.917
loam	1	1.00	-17.0	5.014	-48.0	1.000	106.223	0.000	-10878.8	0.561	0.058	0.553
sand	1	0.01	-1014.0	0.146	-291.6	0.942	0.288	0.436	-621.2	1.262	0.149	1.252
sand	1	0.10	-1122.6	0.115	-113.6	0.407	1.925	0.005	-2351.3	1.179	0.024	1.159
sand	1	1.00	-3.9	0.338	-0.0	1.000	25.887	0.000	-3158.0	0.717	0.005	0.706
clay	5	0.10	-1397.7	0.334	-218.4	0.325	0.395	0.271	-5537.2	1.512	0.196	1.449
clay	5	1.00	-260.6	0.792	-135.3	0.148	1.212	0.013	-6745.0	0.672	0.088	0.687
loam	5	0.10	-5236.5	0.784	-0.0	0.277	2.306	0.100	-8322.9	1.165	0.488	1.157
loam	5	1.00	-1249.5	2.563	-292.9	0.161	28.143	0.001	-8630.0	0.833	0.224	0.838
sand	5	0.10	-918.0	0.190	-556.2	0.432	4.154	0.018	-1273.9	1.612	0.083	1.510
sand	5	1.00	-582.3	0.533	-342.5	0.193	4.888	0.001	-3582.3	1.272	0.012	1.240



**Table 6.** Actual cumulative transpiration predicted by the De Jong van Lier et al. (2013) and all the empirical models for three types of soil (clay, loam and sand) and two levels of root length density  $R$  (medium and high) for the growing season experiment.

Model	Clay		Loam		Sand	
	Medium R	High R	Medium R	High R	Medium R	High R
VLM	46.33	46.51	43.65	43.64	45.56	45.97
PMm	45.79	46.28	43.63	43.75	45.67	46.41
PM	45.68	45.74	43.36	43.34	46.18	46.26
JMII	45.83	46.12	43.59	43.63	45.53	46.32
JMm	45.52	46.11	42.91	43.79	45.29	46.11
JM	45.72	45.10	43.36	43.12	46.00	45.89
FMm	42.66	40.11	42.69	40.81	43.23	41.70
FM	43.48	43.16	42.64	41.61	44.60	44.29



## List of figures

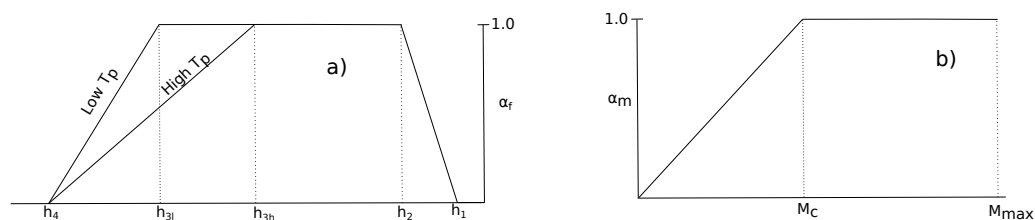


**Figure 1.** a) Feddes et al. (1978) root water uptake reduction function.  $h_2$  and  $h_3$  are the threshold parameters for reduction in root water uptake due to oxygen deficit and water deficit, respectively. The subscripts  $l$  and  $h$  stands for low and high potential transpiration  $T_p$ .  $h_1$  and  $h_4$  are the soil pressure head values above and below which root water uptake is zero due to oxygen and water deficit, respectively. b) Root water uptake reduction function  $\alpha_m$  as a function of matric flux potential  $M$ ;  $M_c$  is the critical value of  $M$  from which the uptake is reduced and  $M_{max}$  is the maximum value of  $M$ , dependent on soil type.

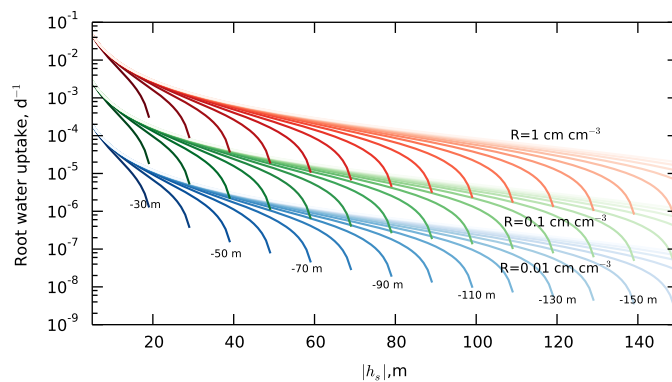


**Figure 2.** Root water uptake  $S$  as a function of soil pressure head  $h_s$  for three values of root length density (0.01, 0.1 and 1.0  $\text{cm cm}^{-3}$ ) and leaf pressure head values ranging from -30 to -200 m by -10 m interval shown by colors gradient (lighter colors indicate lower values and some values are also indicated in the plot). These results were obtained by the analytical solution of eq. 8 given by De Jong van Lier et al. (2013) for a special case of Brooks and Corey (1964) soil. Plant transpiration was set to  $1 \text{ mm d}^{-1}$ , rooting depth to 0.5 m, and the soil and plant hydraulic parameters were taken from De Jong van Lier et al. (2013).



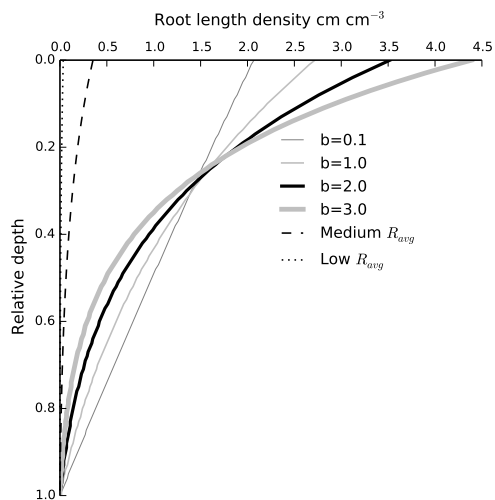


**Figure 3.** Root length density distribution over depth calculated by eq. 28 for several values of  $b$  and  $R_{avg} = 1.0 \text{ cm cm}^{-3}$  and for low and medium  $R_{avg}$  with  $b = 2$ .

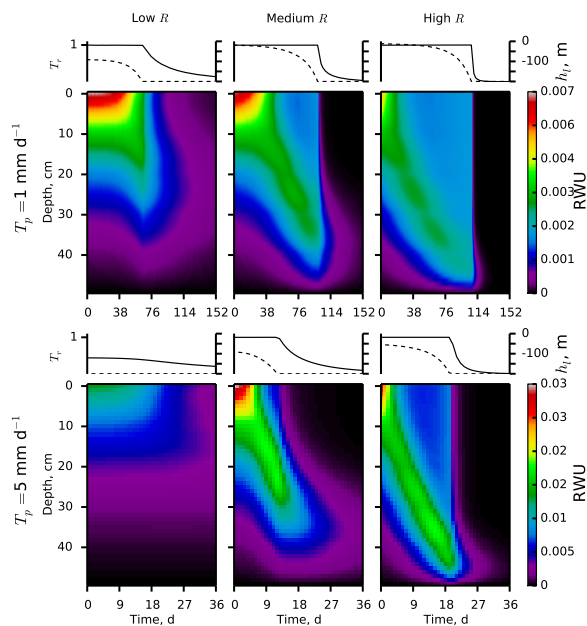


**Figure 4.** Time-depth root water uptake (RWU,  $\text{d}^{-1}$ ) pattern, leaf pressure head ( $h_l$ , dashed line) and relative transpiration ( $T_r$ , continuous line) simulated by SWAP model together with the De Jong van Lier et al. (2013) model for clay soil, two levels of potential transpiration  $T_p$ : 1 and 5  $\text{mm d}^{-1}$  (first and second line of plots, respectively) and three levels of root length density  $R$ : low, medium and high (indicated at the top of the figure).

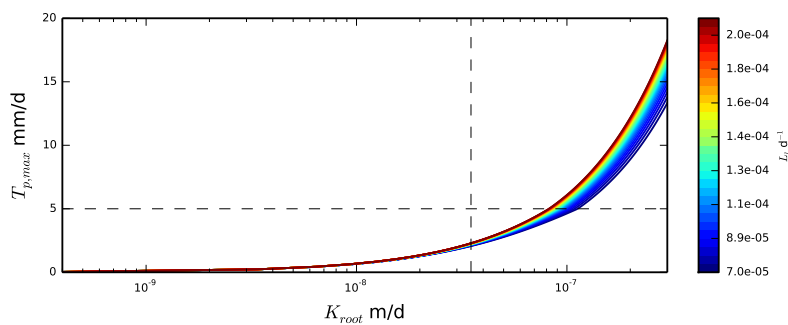


**Figure 5.** Maximum possible transpiration  $T_{p,max}$  as a function of root hydraulic conductivity  $K_{root}$  for some values of the overall conductance over the root-to-leaf pathway  $L_l$  computed by De Jong van Lier et al. (2013) model for rooting depth of 0.5 m, low root length density and constant soil pressure head over depth equals to -1 m for sandy soil. The dashed vertical line highlights the value of  $K_{root} = 3.5 \cdot 10^{-8} \text{ m d}^{-1}$  that was used in our simulations. Horizontal dashed line highlights the value of potential transpiration.

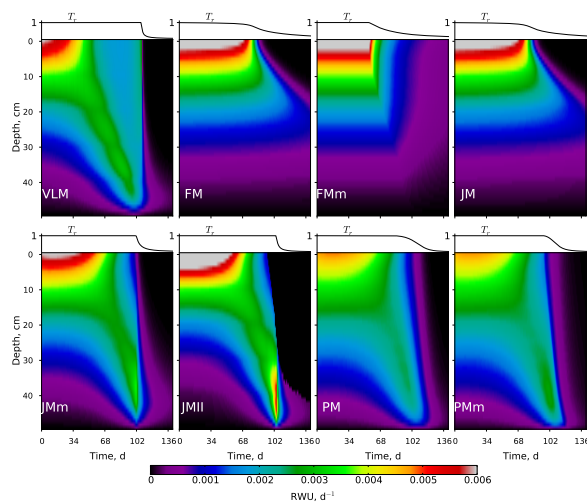


**Figure 6.** Time-depth root water uptake (RWU) pattern and relative transpiration ( $T_r$ ) simulated by SWAP model together with De Jong van Lier et al. (2013) sink and the others empirical models for sandy soil texture, high root length density and  $T_p = 1 \text{ mm d}^{-1}$ .

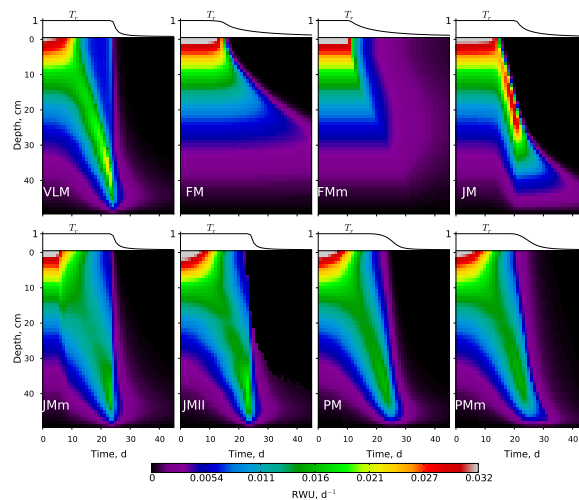


**Figure 7.** Time-depth root water uptake (RWU) pattern and relative transpiration ( $T_r$ ) simulated by SWAP model together with De Jong van Lier et al. (2013) sink and the others empirical models for sandy soil texture, high root length density and  $T_p = 5 \text{ mm d}^{-1}$ .

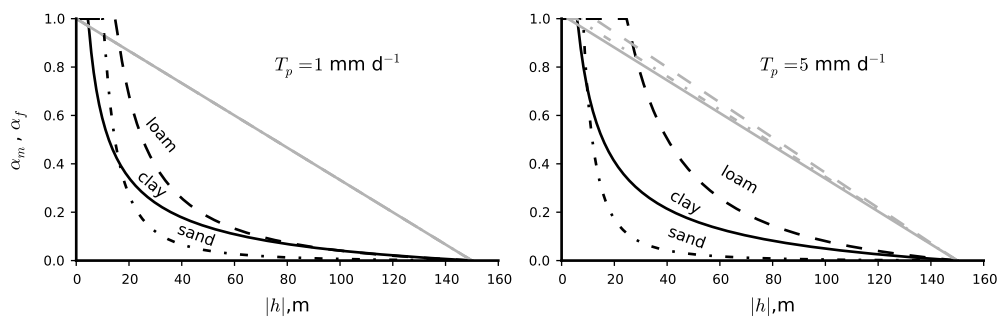


**Figure 8.** Feddes et al. (1978) ( $\alpha_f$ , gray lines) and proposed ( $\alpha_m$ , black lines) water uptake reduction functions as a function of soil pressure head  $h$  using their respective optimized parameters for the scenario of high root length density, three types of soil and two potential transpiration levels.

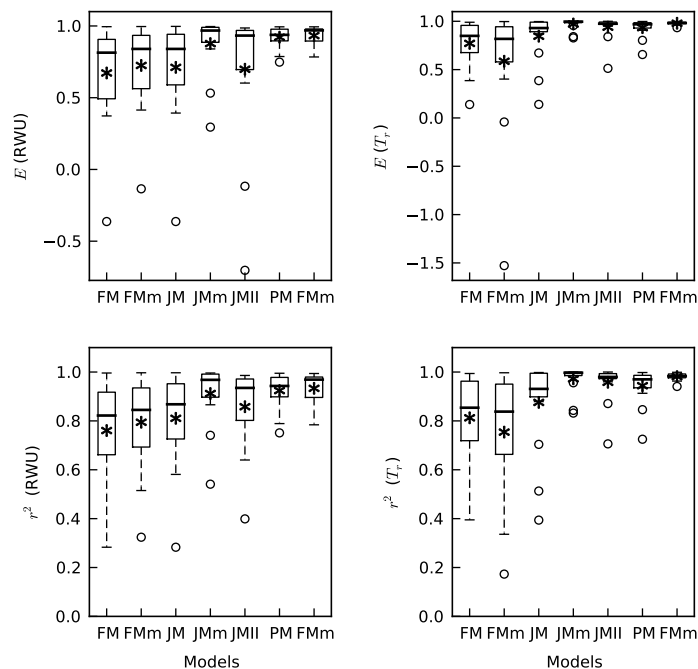


**Figure 9.** Box plot of the coefficient of determination  $r^2$  and model efficiency coefficient  $E$  for the comparison of root water uptake (RWU) and actual transpiration ( $T_a$ ) predicted by each empirical model with the De Jong van Lier et al. (2013) model predictions for the drying-out simulations for three levels of root length density and three types of soil and two potential transpiration levels. The symbols \* and  $\circ$  represent the average and outliers, respectively.



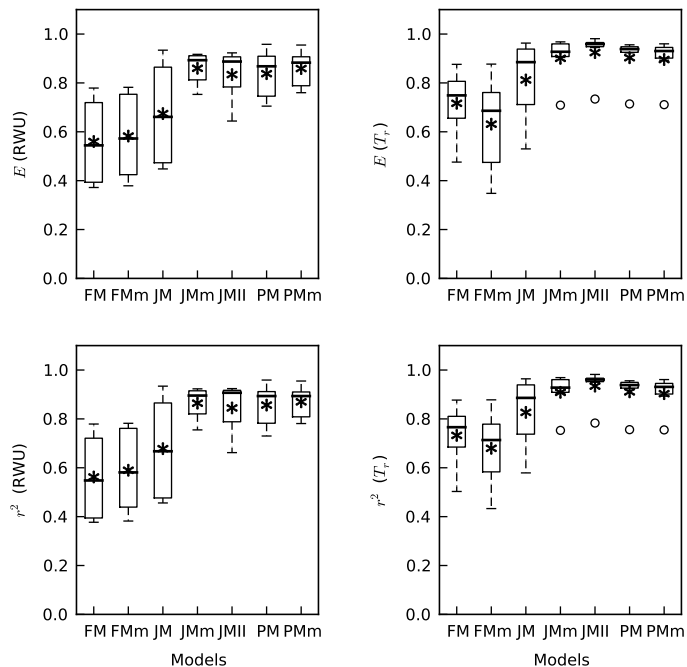


**Figure 10.** Box plot of the coefficient of determination  $r^2$  and model efficiency coefficient  $E$  for the comparison of root water uptake (RWU) and actual transpiration ( $T_a$ ) predicted by each empirical model with De Jong van Lier et al. (2013) model for the growing season experiment for two levels of root length density and three types of soil. The symbols \* and  $\circ$  represent the average and outliers, respectively.